Supplemental Information for:

Coupled Mg/Ca and clumped isotope analyses of foraminifera provide consistent water temperatures

Sebastian F.M. Breitenbach[1,*], Maryline J. Mleneck-Vautravers[1], Anna-Lena Grauel[1,§], Li Lo[1,#], Stefano M. Bernasconi[2], Inigo A. Müller[2], James Rolfe[1], Fernando Gázquez[1], Mervyn Greaves[1], David A. Hodell[1]

[1]Godwin Laboratory for Palaeoclimate Research, Department of Earth Sciences, University of Cambridge, United Kingdom
[2]Geological Institute, ETH Zurich, Zurich, Switzerland
*now at Sediment- & Isotope Geology, Ruhr-Universität Bochum, Germany
[§]now at the Institute of Applied Geosciences, Graz University of Technology, Graz, Austria
[#]now at State Key Laboratory of Isotope Geochemistry, Guangzhou Institute of Geochemistry, Chinese Academy of Sciences, China

List of Supplemental Material

Estimating the effect of changes in $\delta^{18}O$ and Δ_{47}

The task is to find $\delta^{18}O_{sw}$ as a function of $\delta^{18}O_{cc}$ ($f(\Delta_{47},\delta^{18}O_{cc})$) using

$$T = m_2 + 1/S_0\,(\delta^{18}O_{cc} - \delta^{18}O_{sw}) + 1/S_0\,(\delta^{18}O_{cc} - \delta^{18}O_{sw})^2 \qquad (1)$$

and

$$\Delta_{47} = (S_{\Delta 47}/T^2) + \text{const.} \qquad (2)$$

For this we consider only small changes of T, Δ_{47}, and $\delta^{18}O_{cc}$, because then we can simplify eqs. (1) and (2). For small changes in T and $\delta^{18}O_{cc}$, it would be enough to consider only the linear part in eq. (1), which then becomes

$$T = m_2 + 1/S_0\,(\delta^{18}O_{cc} - \delta^{18}O_{sw}) \qquad (3)$$

Small changes can then be calculated simply as

$$\Delta T = 1/S_0\,(\Delta\,\delta^{18}O_{cc} - \Delta\,\delta^{18}O_{sw}) \qquad (4)$$

which results in

$$\Delta\, \delta^{18}O_{sw} = \Delta\, \delta^{18}O_{cc} - S_0\, \Delta T \qquad (5)$$

To find the effect of small changes in $\delta^{18}O_{sw}$ due to small changes in Δ_{47} is not so simple as for eq. (1), because the dependence on T is not linear, but $1/T^2$. Therefore, we need to apply a Taylor expansion on eq. (2) which results in

$$\Delta\,\Delta_{47} = - S\Delta_{47}\, (2/T^3)\, \Delta T, \text{ or } \Delta T = - (\Delta\,\Delta_{47}\, T^3/2S_{\Delta 47}) \qquad (6)$$

Replacing ΔT in eq. (5) we finally get

$$\Delta\delta^{18}O_{sw} = \Delta\delta^{18}O_{cc} + (S_0/S\Delta_{47})\, (T^3/2)\, \Delta\,\Delta_{47} \qquad (7)$$

From these last equations it should be clear that the nonlinear nature of the relationship between Δ_{47} and T causes a temperature dependent factor. Still, selecting a certain value for T, i.e., T = 300 K, small changes in T and, hence, in Δ_{47} cause a linear response. Here the range of change in Δ_{47} can be between 0.5‰ and 0.8‰.

Comparison of $T_{\Delta 47}$ and $T_{Mg/Ca}$ with Atlas-based SST and calcification depth temperatures

To test if the reconstructed temperatures ($T_{\Delta 47}$ and $T_{Mg/Ca}$) agree with modern data, we plot them against GISS-Atlas (NODC_WOA98, http://data.giss.nasa.gov) derived SST and calcification depth temperatures (Fig. S2). $T_{\Delta 47}$ and $T_{Mg/Ca}$ are compared with annual mean temperatures at the estimated calcification depth (T_{calc}) of the different foraminifera species and at the sea surface (T_{sst}), with T_{calc} and T_{sst} data derived from the GISS Atlas (NODC_WOA98). $T_{\Delta 47}$ agree well with annual mean temperature estimates for calcification depths, but show higher scatter when compared to SST estimates (Figs. S2a, b). These observations support the notion that clumped isotope signal reflects the temperature at the time and depth of test calcification.

$T_{Mg/Ca}$ estimates are seemingly too high when compared to annual temperature at the estimated calcification depth (Figs. S2c), whereas they are closer to the mean annual sea surface temperature (Figs. S2d), even though the scatter increases. This observation could be explained by a combination of the following factors:

i) Calcification depths are notoriously difficult to define and thus might not be correctly assigned (Pearson 2012). If calcification occurred mainly in lower water depths, the calcification depth estimate might result in too high temperatures. However, the fact that $T_{\Delta 47}$ agrees well with calcification depth estimates (Fig. S2a) suggests that calcification depths are correctly assigned. Thus, calcification depth estimates are likely correct.

ii) Mg/Ca might be elevated due to addition of Mg via crust formation (Fehrenbacher et al. 2017), or during gametogenesis (Nürnberg et al. 1996, Sadekov et al. 2005, Fehrenbacher et al. 2017) or contamination (Lea et al. 2005). Addition of such Mg would lead to erroneous $T_{Mg/Ca}$ estimates.

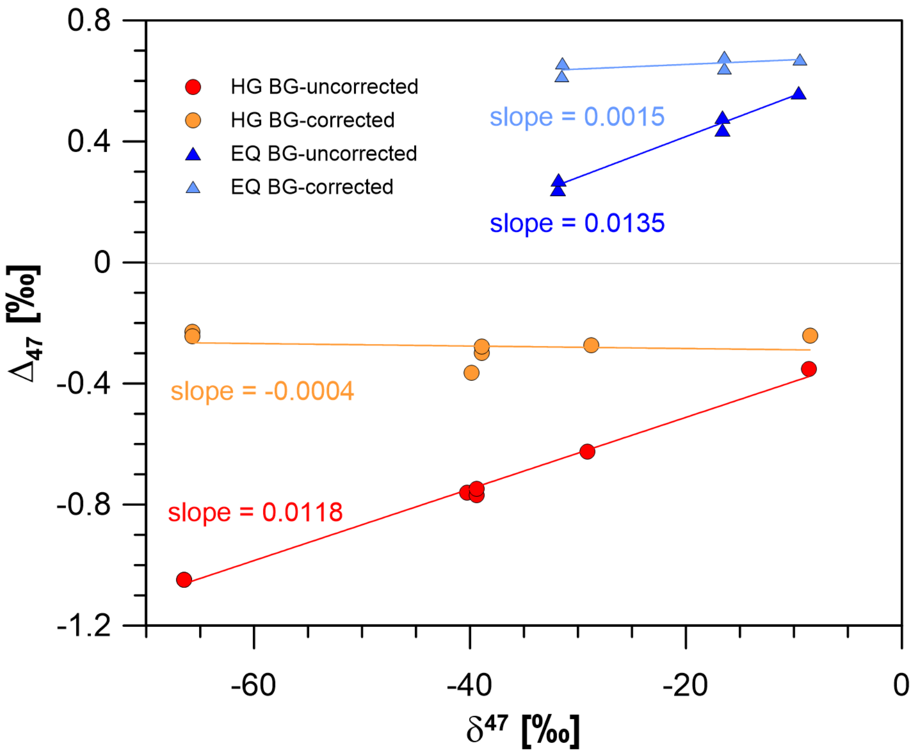

Figure S1. Visualization of the effectiveness of the PBL correction determined by monitoring the backgrounds on all cups before each run. This correction effectively eliminates the slope of the heated (HG, 1000°C) and equilibrated (EQ, 24.9°C) gas lines, as illustrated here for data collected from January-February 2016.

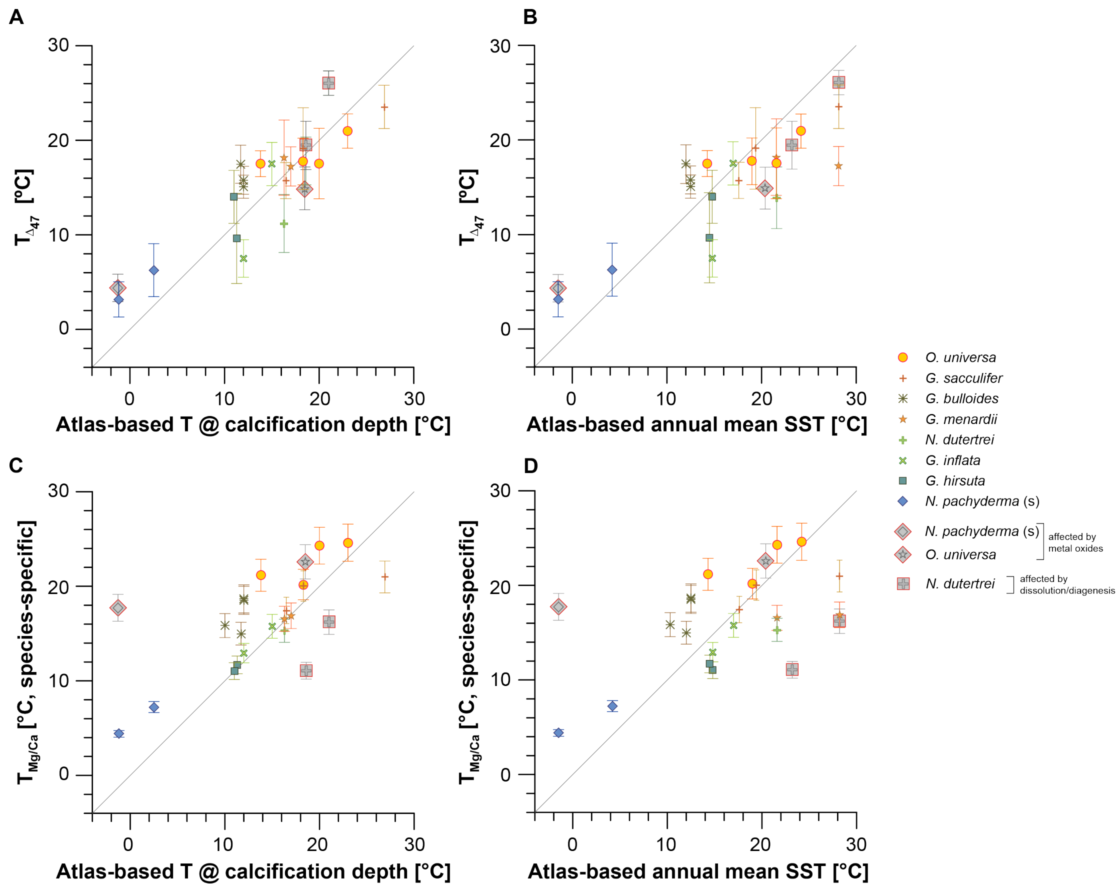

Figure S2. Comparison of reconstructed temperatures ($T_{\Delta 47}$ and $T_{Mg/Ca}$) with GISS Atlas data (NODC_WOA98). **A**) $T_{\Delta 47}$ vs Atlas derived temperatures at calcification depth. **B**) Same as A, but with GISS Atlas based SST estimates. **C**) $T_{Mg/Ca}$ is shown against Atlas derived calcification depth temperature. **D**) Same as B, but with $T_{Mg/Ca}$. Samples identified as being affected by diagenesis, dissolution, or metal oxide coating/filling are highlighted by grey symbols. Metal oxides do not significantly affect $T_{\Delta 47}$ estimates as confirmed by the agreement between calcification depth temperature and SST (figures A and B), whereas $T_{Mg/Ca}$ estimates are strongly offset (figures C and D). Diagenesis effects can affect both, $T_{Mg/Ca}$ and $T_{\Delta 47}$.

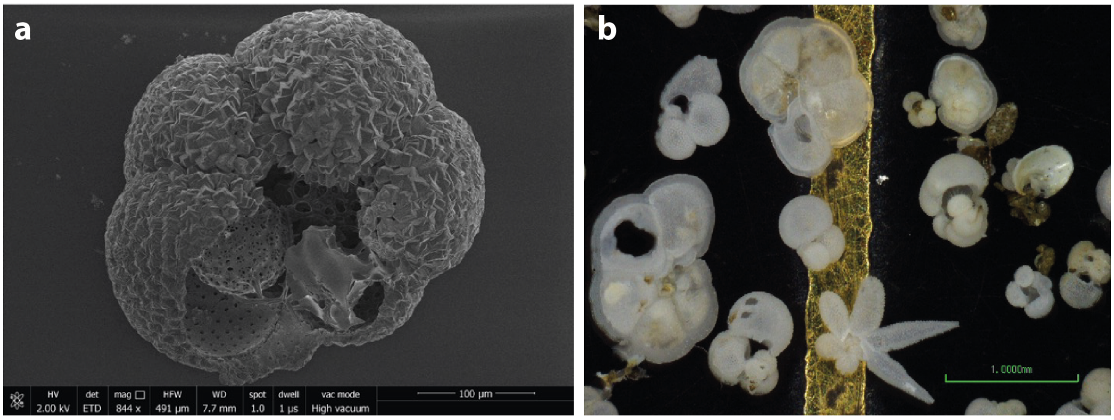

Figure S3. a) Example of dissolution in *N. dutertrei* from sample IODP1436C-1H1W_25cm, Pacific Ocean, where the calcite saturation depth is much shallower compared to the Atlantic. Samples from this site have been reported to suffer extensive dissolution at 1700 water depth (Tamura et al. 2015). Here we document dissolution of umbilical teeth and the last chamber on the generally dissolution resistant *N. dutertrei* sample. This sample falls below the tandem line. **b)** Carbonate dissolution on a number of very delicate and lightly-calcified tests of planktonic foraminifers (*G. menardii* and *G. sacculifer*) from core MD 77-191, showing initial signs of supra-lysoclinal dissolution as evidenced by holes in some final chambers.

Comparison of selected calibrations

The table below gives the slopes and intercepts for selected calibrations, projected to 25°C.

Reference	**Slope**	**Intercept**
Ghosh et al. (2006)	0.062	0.021
Kelson et al. (2017) (Eq. 2)	0.0422±0.0013	0.215±0.014
Bonifacie et al. (2017) (global)	0.0422±0.0019	0.218±0.0207
Kele et al. (2015) original	0.044±0.005	0.207±0.047
Kele et al. (2015) fully recalculated	0.0449±0.001	0.167±0.01
Cambridge (this study)	0.0447±0.006	0.149±0.07

Supplemental References

Tamura Y., Busby C. J., Blum P., and the Expedition 350 (2015) Scientists *Proceedings of the International Ocean Discovery Program, Expedition 350*: Izu-Bonin-Mariana Rear Arc: College Station, TX (International Ocean Discovery Program). doi./10.14379/iodp.proc.350.2015.

NODC_WOA98, data provided by the NOAA/OAR/ESRL PSD, Boulder, Colorado, USA, http://www.esrl.noaa.gov/psd/